Electronic Supplementary Material (ESI) for Nanoscale.

Supplementary Information

Preparation, Optical and Electrical Properties of PTCDA Nanostructures

Yuyan Han,[a] Wei Ning,[a] Haifeng Du,[a] Jiyong Yang,[a] Ning Wang,[a] Liang Cao,[a] Feng Li,[a] Fapei Zhang,[a] Faqiang Xu*,[b] and Mingliang Tian*,[a]

[a.]High Magnetic Field Laboratory, Chinese Academy of Science, Hefei 230031, Anhui, People's Republic of China

[b.]National Synchrotron Radiation Laboratory, School of Nuclear Science and Technology, University of Science and Technology of China, 42 Hezuohua Road, Hefei 230029, Anhui, People's Republic of China.

*Corresponding authors, Prof. FaQiang Xu, E-mail: fqxu@ustc.edu.cn

Prof. MingLiang Tian, E-mail: tianml@hmfl.ac.cn

1. Preparation and the morphology characteristics of AAO used as substrates

The porous anodic alumina oxide (AAO) were prepared by a two-step anodizing process in oxalic acid ($H_2C_2O_4$) solution. Firstly, the high purity (99.999%) aluminum foils were annealed at 500 ºC for 10 h in muffle in air atmosphere, and then cooled down naturally in order to release the stress generated during machining process of aluminum foil. The foils were degreased in acetone ultrasonically, and then polished electrochemically in a mixture of sulfuric (5 vol%), phosphoric (95 vol%) and chromic acids (20 $g.L^{-1}$) under 20 V_{dc} till the surface become shinny smooth. The polished aluminum foils were anodized in 2 ºC, 0.3 M $H_2C_2O_4$ solutions under constant voltage (40 *V*) for 6 h. Subsequently, the formed alumina was dissolved by a mixture solution of phosphoric (6.0 wt%) and chromic acid (1.8 wt%) at 60 ºC. Then, the aluminum foil was anodized again for 10 h under the same conditions as the first step. To obtain the transparent AAO, the remaining aluminum was removed using the saturated solution of $CuCl_2$. Then the transparent AAO were cleaned in deionized water ultrasonically and blow-dry by high purity nitrogen (N_2).

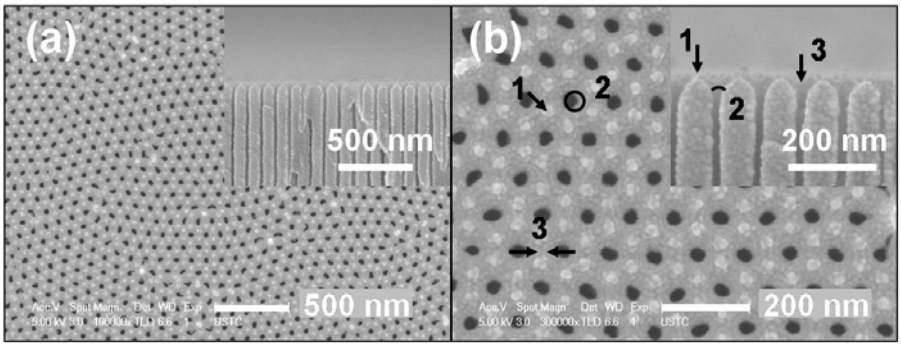

Figure S1. Low magnified (a) and enlarged (b) SEM images of AAO film annealed at 360 ºC in UHV chamber (the insets are the images of the cross-sectional areas).

From Figure S1, the pore diameter and the distance between the adjacent pore centers

are about 35 and 100 nm respectively. The active sites with smaller curvature radius forming at the AAO surface and the pore openings are pointed out by the black arrows and circles (site 1: the connection point of three adjacent pores; site 2: the pore opening; site 3:the ridge of the two joint pores). Because the AAO has the good thermal stability, the annealing process does not change the morphology of AAO.

2. Images of the annealed AAO and the AAOs with PTCDA NSs

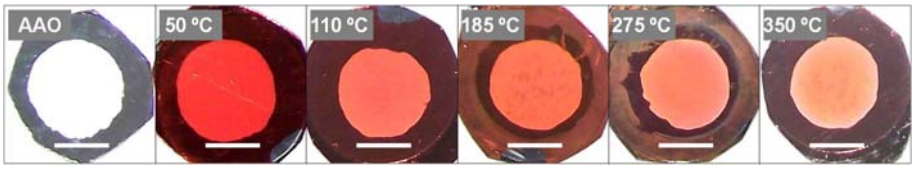

Figure S2. Optical images of the AAO annealed and those deposited by PTCDA molecules at different T_s.

The AAO annealed at 360 ºC in VHU chamber is still transparent for visible light. When the PTCDA was deposited on the AAO at different T_s, colors of the samples varies from red to orange gradually.

3. SEM and TEM images of NRs

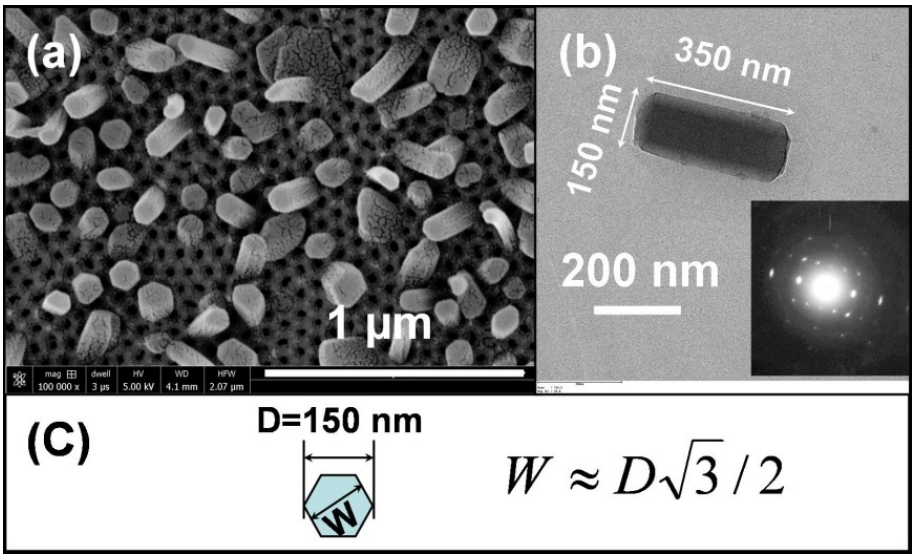

Figure S3. (a) SEM image of NRs growing on AAO at T_s = 185 ºC; (b) the TEM image and SAED pattern of a single NR; (c) illustration of the relationship between the width and the diagonal length of the NR.

It was seen clearly from Figure S3 (a) that the majority of NRs were grown from the pore openings and are hexagonal prisms; the TEM image of the isolated NR in Figure S3 (b) indicates that the surface of the NR is very smooth, and the length of the NR is about 350 nm with a width of about 130 nm calculated from the formula of $W \approx 150\sqrt{3}/2$, as shown in (c). the SAED pattern in the inset of Fig.S3 (b) indicates that the NR is single-crystal.

4. Images of SEM, TEM and SAED of PTCDA NWs

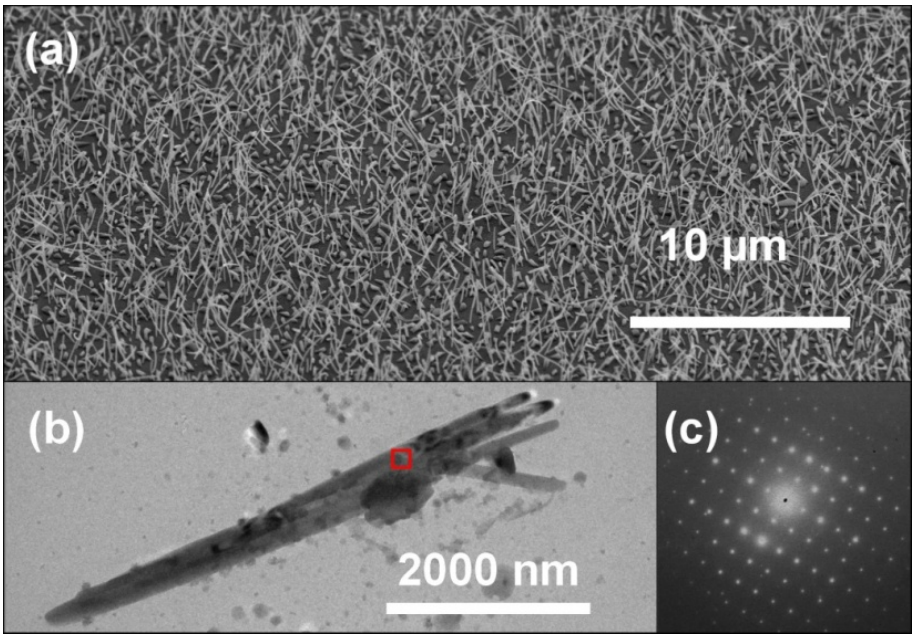

Figure S4. (a) SEM image of the NWs growing on AAO (45 º tilted) at T_s = 275 ºC; (b) TEM image of a bunch of NWs; (c) SAED pattern of the NW.

It was shown that the NWs grown on AAO surface have a typical length of 5 μm and a diameter of 70 nm, indicating a large aspect ratio; the SAED pattern confirms its high single-crystal quality.

5. Cross section images of the samples prepared at T_s = 350 ºC

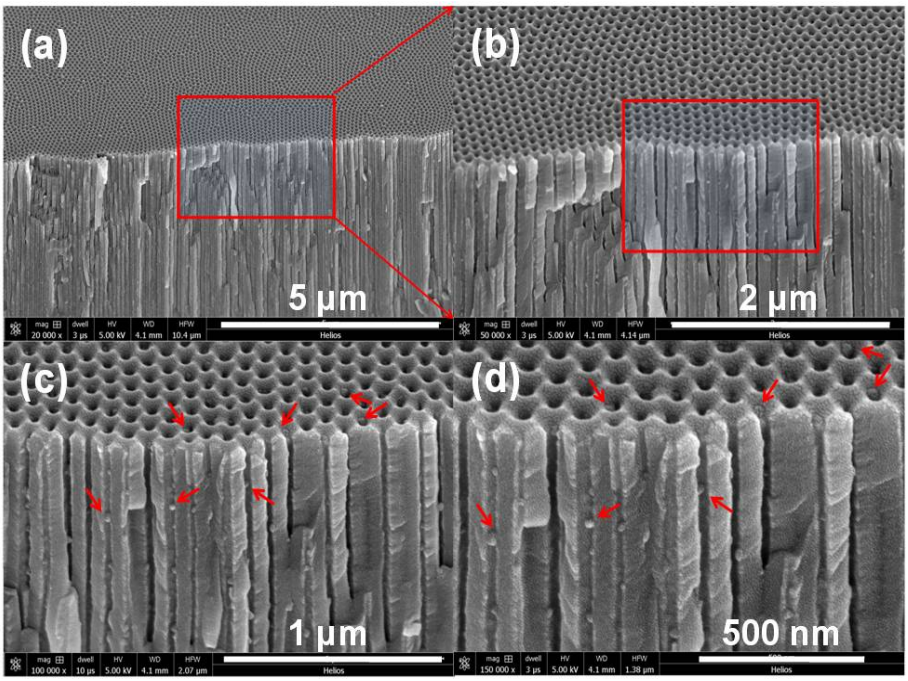

Figure S5. (a), (b) are respectively the SEM images of the cross-section of AAO with different magnifications that the NPs were grown at T_s = 350 ºC. The red arrows point out the typical NPs formed at the pore openings and in nanochannels of AAO. (c), (d) are the blow-up of the marked areas in (a) and (b), respectively. .

It was shown that no NRs and NWs can be seen. However, the NPs were seen inside the pores from the enlarged plots.

6. Comparison between the current versus voltage (*I-V*) curves of SiO_2 dielectric layer and PTCDA NW.

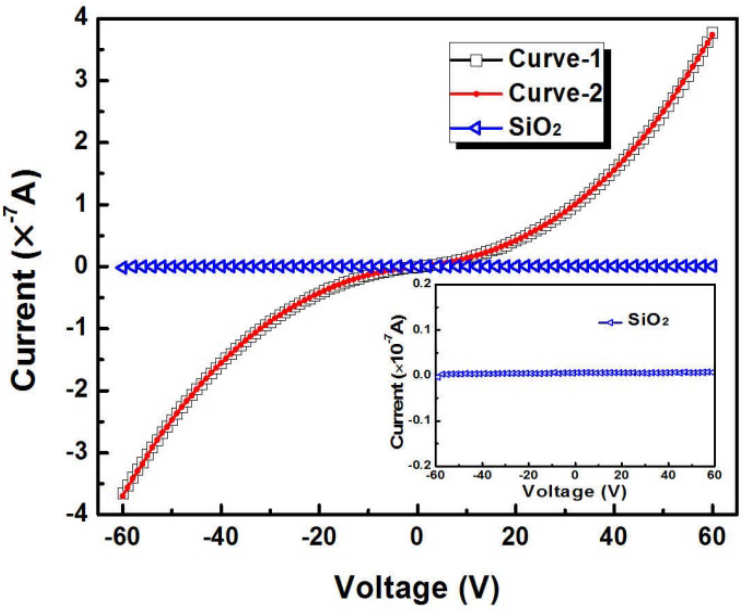

Figure S6. I-V curves of SiO_2 dielectric layer and PTCDA NW.

It was seen that the *I-V* curve of SiO_2 dielectric layer between Pt electrode and Si substrate is almost insulating behavior without current flow within the scanning range of the voltage from -60 V to 60 V, indicating the FIB deposition of Pt electrodes has less effect on the SiO_2 dielectric layer. This will ensure the reliability of the electrical properties of PTCDA NW.